

## **Coating of Iron Oxide Nanoparticles with Human and Bovine Serum Albumins: A Thermodynamic Approach**

M. Keshavarz<sup>1,2\*</sup> and Z. Ghasemi<sup>2</sup>

<sup>1</sup> Department of Chemistry, Shahreza Branch, Islamic Azad University, Shahreza, Isfahan, Iran

<sup>2</sup> Department of Chemistry, Dolatabad Branch, Islamic Azad University, Dolatabad, Isfahan, Iran

Received April 2011; Accepted June 2011

### **ABSTRACT**

In this research, the Magnetite nanoparticles ( $\text{Fe}_3\text{O}_4$ ) were prepared by coprecipitation of  $\text{Fe}^{3+}$  and  $\text{Fe}^{2+}$  solution in alkaline medium. Two kinds of surfactants, cetyl tri methyl ammonium bromide (CTAB) and cetyl pyridinium chloride (CPC) were used in the synthesis.  $\text{Fe}_3\text{O}_4$  Nanoparticles were coated with human serum albumin (HSA) and bovine serum albumin (BSA). Characteristics of coated magnetic nanoparticles and no coated were carried out using scanning electron microscopy, X-ray diffraction and FT-IR spectroscopy. The interactions of colloidal iron oxide nanoparticles with serum albumins, including BSA and HSA, were investigated by UV-Vis spectroscopy at process different pH and temperatures. The thermodynamic parameters of coating were obtained from Van't Hoof equation. The results revealed that both  $\Delta H^\circ$  and  $\Delta S^\circ$  of reactants positive values. These results also demonstrate that pH can play an important role on adsorption of proteins on iron oxide nanoparticles.

**Keywords:** iron oxide nanoparticles;  $\text{Fe}_3\text{O}_4$ ; human serum albumin (HSA); bovine serum albumin (BSA)

### **INTRODUCTION**

Nanoscience is one of the most important research and development in modern science [1, 2]. The development of a wide of superparamagnetic magnetite nanoparticles has shown great promise for various biomedical and biotechnological applications, for example magnetic resonance imaging contrast enhancement, hyperthermia, drug delivery, bioseparation [3-11].

The advantage of using iron oxide nanoparticles relies on their chemical stability, in contrast to Fe metal nanoparticles. Because of the widespread applications of magnetic nanoparticles (MNPs), in biomedical and biotechnology much attention has been paid to the preparation of different kinds of MNPs. Iron oxide nanoparticles prepared by classical methods Recently, of Fe precursors in solution salts containing surfactants has been developed

for the synthesis of discrete and monodisperse superparamagnetic iron oxide nanoparticles (SPIONs). The synthesis of nanoparticles with controllable sizes is very important to characterize the size-dependent physical properties of nanoparticles. A number of preparation methods for MNPs have been developed, such as chemical coprecipitation, microemulsion, thermal decomposition, electrochemistry and sol-gel methods [12- 18].

In the absence of any surface coating, magnetic iron oxide particles have hydrophobic surfaces with a large surface area to volume ratio. Due to hydrophobic interactions between the particles, these particles agglomerate and resulting in increased particle size. In the course of much attention has been focused on the encapsulation of magnetic nanoparticles with specific materials such as inorganic and organic materials. In study we used two kind of surfactant: CPC and CTAB and we applied BSA and HSA for encapsulation of magnetic

\* Corresponding author: keshavarz@iaush.ac.ir; dmekeshavarz@yahoo.com

nanoparticles because they have biocompatible and biodegradable properties as well as low toxicity. BSA has been one of the most extensively studied proteins and HSA is the most abundant protein in blood plasma and it is also the principal factor contributing to the colloid osmotic pressure of the blood [19, 20].

Our report described a detailed investigation on interactions of MNPs bound to biological host models: BSA and HSA. We demonstrate that BSA and HSA are suitable for coated iron oxide nanoparticles.

## EXPERIMENTAL

### Materials

The chemical reagents used in this work were  $\text{FeCl}_2 \cdot 4\text{H}_2\text{O}$ ,  $\text{FeCl}_3 \cdot 6\text{H}_2\text{O}$ , ammonium hydroxide ( $\text{NH}_3 \cdot \text{H}_2\text{O}$ ), CTAB and CPC surfactant. BSA and HSA were purchased from Merck and Sigma-Aldrich. Distilled water was used for preparation of the solutions after deoxygenating with dry  $\text{N}_2$ .

### Synthesis of $\text{Fe}_3\text{O}_4$ nanoparticles

First, (0.01 mol)  $\text{FeCl}_2 \cdot 4\text{H}_2\text{O}$  and (0.02 mol)  $\text{FeCl}_3 \cdot 6\text{H}_2\text{O}$  were dissolved in 25 mL distilled water; aqueous ammonium hydroxide solution (1.5 mol/L) was also prepared. Then, surfactant solution (CTAB or CPC) was added to the former solutions to obtain Precursor solution II and Precursor solution I. Second, Precursor solution I was added into Precursor solution II drop wise with strong stirring under the protection of dry nitrogen at the desired temperature. Just after mixing the solutions, the color of the solution changed from light brown to black, indicating the forming of  $\text{Fe}_3\text{O}_4$  nanoparticles, which was allowed to crystallize completely for another 60 min under rapid stirring. The precipitate  $\text{Fe}_3\text{O}_4$  nanoparticles were washed by repeated cycles of centrifugation and redispersion in distilled water. Washing was performed for five times with distilled water. Third, the precipitate  $\text{Fe}_3\text{O}_4$  nanoparticles were redispersed in the same surfactant solution under the conditions of ultrasonic agitation for 30 min and strong stirring for another 40 min. The products ( $\text{Fe}_3\text{O}_4$  nanoparticles) were also washed by repeated

cycles of centrifugation and redispersion in distilled water. The washing was performed four times with distilled water. The final products were dried in a vacuum oven at room temperature for 24 h, and the  $\text{Fe}_3\text{O}_4$  nanoparticles were finally obtained.

### Preparation of coated iron oxide NPs with bovine serum albumin

1 g bovine serum albumin (BSA), which was dissolved in 20 mL water, was added to the NP precursor under the nitrogen gas. Then the reaction mixture was sonicated (using an Aquasonic ultrasonic cleaner) for 2.5 h. A clear reddish-brown color solution was formed. Excess BSA was removed by ultracentrifugation at 15 000 rpm for 30 min.

### Human serum albumin coated iron oxide NPs synthesis

20 mL of colloid solution of  $\text{Fe}_3\text{O}_4$  prepared was diluted to 100 mL which surged with ultrasonic for 30 min; the colloid solution was filtrated with qualitative filter paper to get colloid solution with  $\text{Fe}_3\text{O}_4$  nanoparticles less than 100 nm. At about  $40^\circ\text{C}$  under ultrasonic, proper amounts of HSA were added into the colloid solution, with stirring for 1h. The coated  $\text{Fe}_3\text{O}_4$  with HAS was obtained finally.

### Interaction of MNPs and BSA and HSA

25 mL of 10 ppm BSA or HSA solution and 0.001 g magnetic nanoparticles were transferred to the beaker and allowed the interaction to be completed for 3 hour under rapid stirring. The coated NPs separated were by centrifugation. The adsorption of proteins on the surface of nanoparticles was studied by UV-Vis spectroscopy. The interactions processes were performed at various pH (8, 9, 10, 11, 12) and temperatures (293.15K, 303.15K, and 313.15K). The concentration of free protein, was determined by measuring the absorption of solution at 280nm. [21, 24].

The adsorption data were analyzed in other to calculate the binding parameters using SQUAD program. This program is designed to calculate the best value for the stability constant of the proposed equilibrium model by employing non-linear least square approached. The results of adsorption measurements are shown in table 1-3.

**Table 1.** Summary of the adsorption of BSA and HSA on MNPs at 293.15 K after 3h

HSA		BSA	
pH	adsorption $\lambda = 220\text{nm}$	pH	Adsorption $\lambda = 280\text{nm}$
8	2.235	8	1.660
9	2.133	9	1.531
10	1.511	10	1.501
11	1.105	11	1.435
12	0.759	12	0.627

**Table 2.** Summary of the adsorption of BSA and HSA on MNPs at 303.15 K after 3h

HSA		BSA	
pH	Adsorption $\lambda = 220\text{nm}$	pH	Adsorption $\lambda = 280\text{nm}$
8	2.483	8	1.765
9	2.402	9	1.630
10	1.860	10	1.431
11	1.189	11	1.233
12	0.958	12	0.775

**Table 3.** Summary of the adsorption of BSA and HSA on MNPs at 313.15 K after 3h

HSA		BSA	
pH	Adsorption $\lambda = 220\text{nm}$	pH	Adsorption $\lambda = 280\text{nm}$
8	2.869	8	1.789
9	2.749	9	1.603
10	2.562	10	1.583
11	2.331	11	1.478
12	1.423	12	1.408

## ANALYTICAL METHODS

### X-ray diffraction (XRD)

The  $\text{Fe}_3\text{O}_4$  nanoparticles were analyzed for phase composition using X-ray powder diffractometer (XRD, Bruker D8 Advance Germany) over the  $2\theta$  range from 20-80 at the rate  $2.5\theta/\text{min}$ . ( $\theta = 1.5406$ ).

Fig. 1 shows the X - ray diffraction (XRD)

pattern of uncoated  $\text{Fe}_3\text{O}_4$  nanoparticles. The six characteristic peaks occurred at  $2\theta = 30.09, 35.42, 43.05, 56.94$  and  $62.14$ , which were marked by their corresponding indices (220), (311), (400), (422), (511) and (440), respectively. Magnetic nanoparticles were synthesis with CPC and CTAB surfactant but their XRD pattern aren't different.

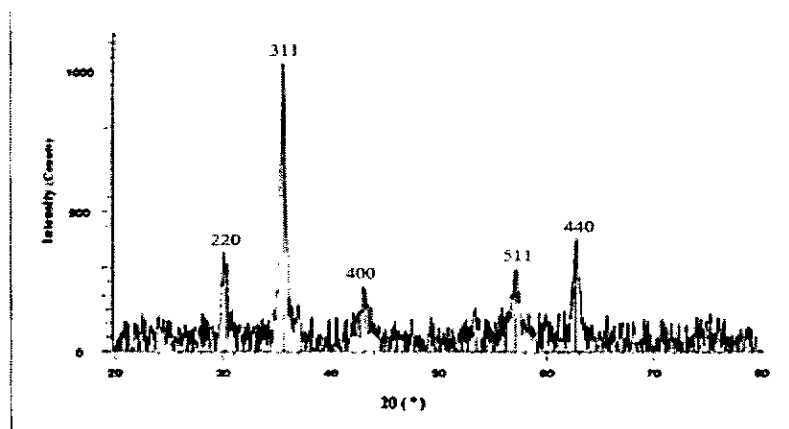


**Fig. 1.** XRD pattern of  $\text{Fe}_3\text{O}_4$  nanoparticles.

Fig.2 shows the X-ray diffraction (XRD) pattern of coated  $\text{Fe}_3\text{O}_4$  magnetic nanoparticles with BSA and HSA. XRD pattern revealed that

the prepared magnetic nanoparticles were pure  $\text{Fe}_3\text{O}_4$  [21, 22].

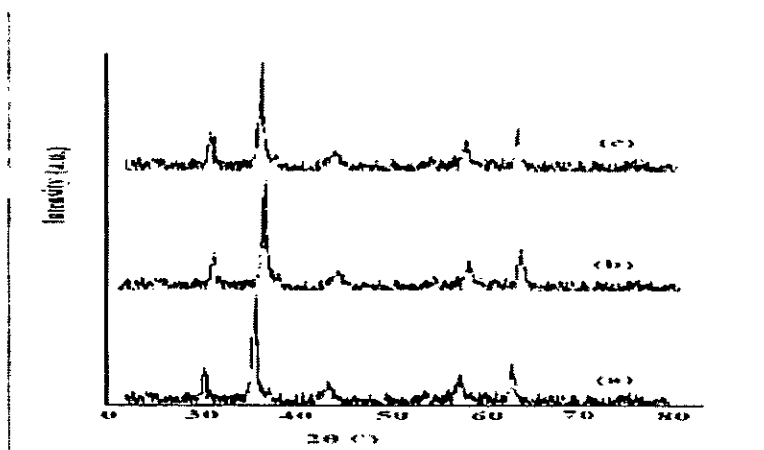


Fig. 2. a) XRD pattern of  $\text{Fe}_3\text{O}_4$  nanoparticles b) XRD  $\text{Fe}_3\text{O}_4$  nanoparticles coated with HSA and c) XRD  $\text{Fe}_3\text{O}_4$  nanoparticles coated with BSA.

### Scan Electron Microscopy (SEM)

The morphology and size of the synthesized particles were investigated using scan electron microscope (SEM, Philips XL30, SE detector). The SEM photograph of the prepared iron oxide nanoparticles are shown Fig.3 and 4. These similar to the typical SEM image of uniform  $\text{Fe}_3\text{O}_4$  nanoparticles Fig.3 and 4 are correspond to the SEM images of magnetite NP prepared

with CPC and CTAB, respectively. It can be deduced from Fig. 5 and Fig. 6 the distribution of particle size is very narrow. The mean diameter of NPs is less than 100 nm, which was bigger than the naked  $\text{Fe}_3\text{O}_4$  nanoparticles. The size difference was demonstrated that the BSA and HSA was coated on  $\text{Fe}_3\text{O}_4$  nanoparticles successfully again [21, 22].



Fig. 3. SEM images of  $\text{Fe}_3\text{O}_4$  nanoparticles with CTAB surfactant.

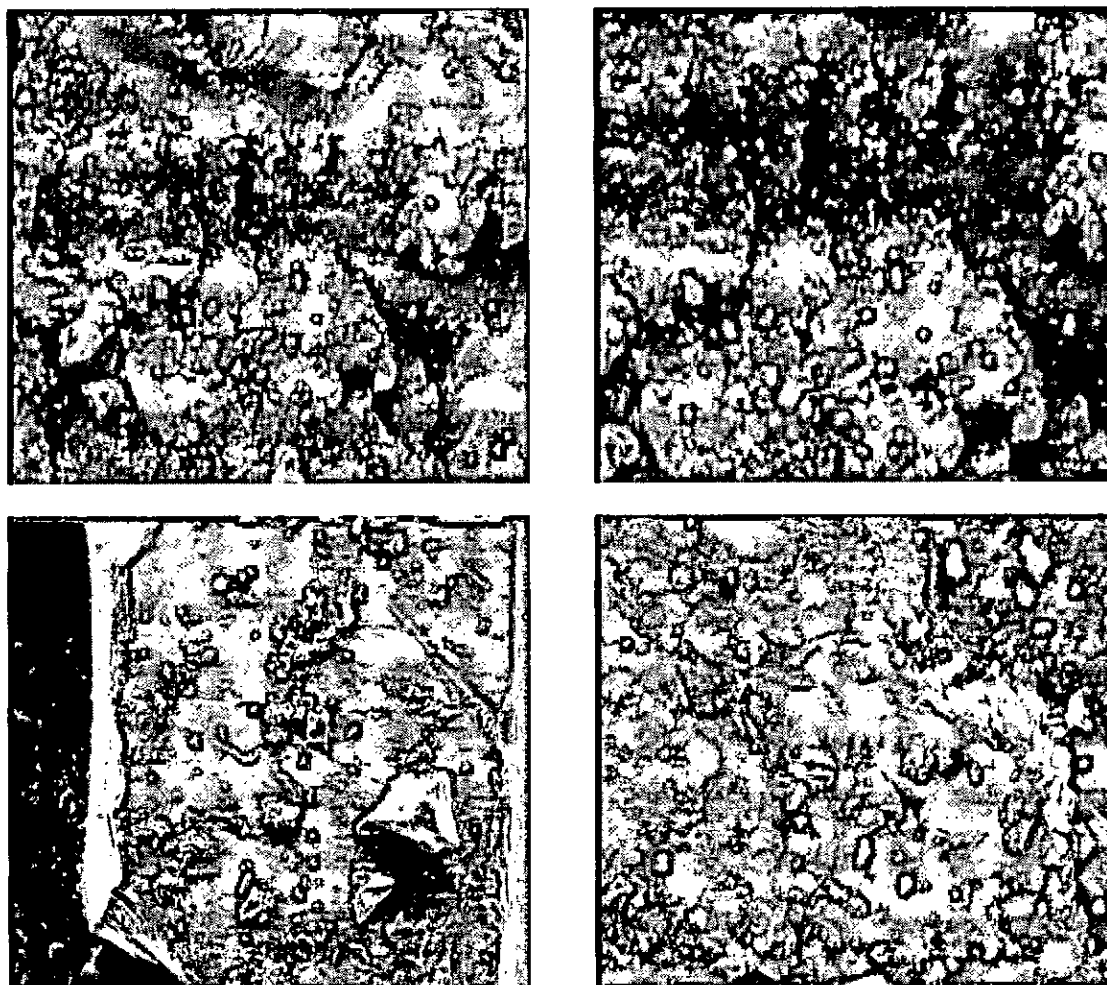


Fig. 3. Continued.



Fig. 4. SEM images of  $\text{Fe}_3\text{O}_4$  nanoparticles with CPC surfactant.

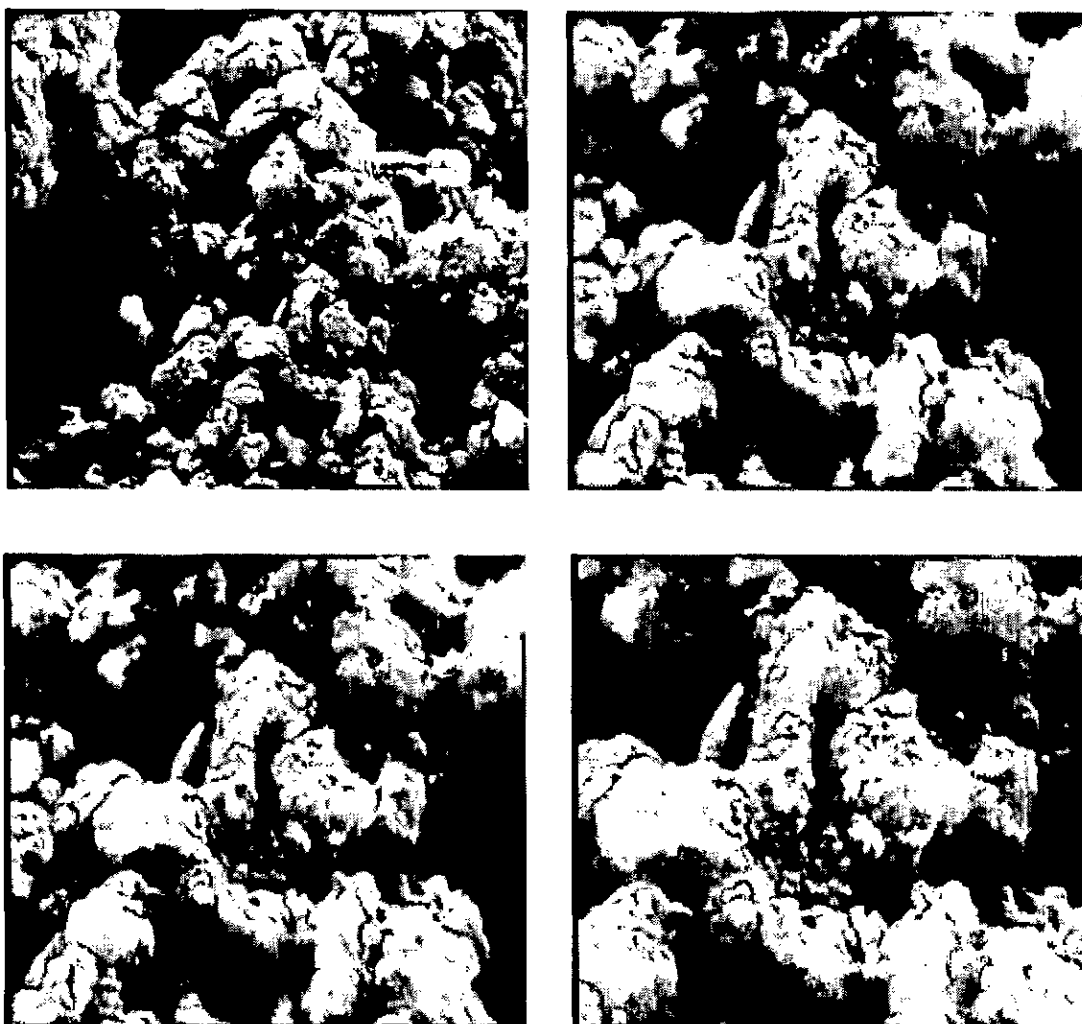


Fig 5. SEM images of Fe<sub>3</sub>O<sub>4</sub> nanoparticles coated with BSA.

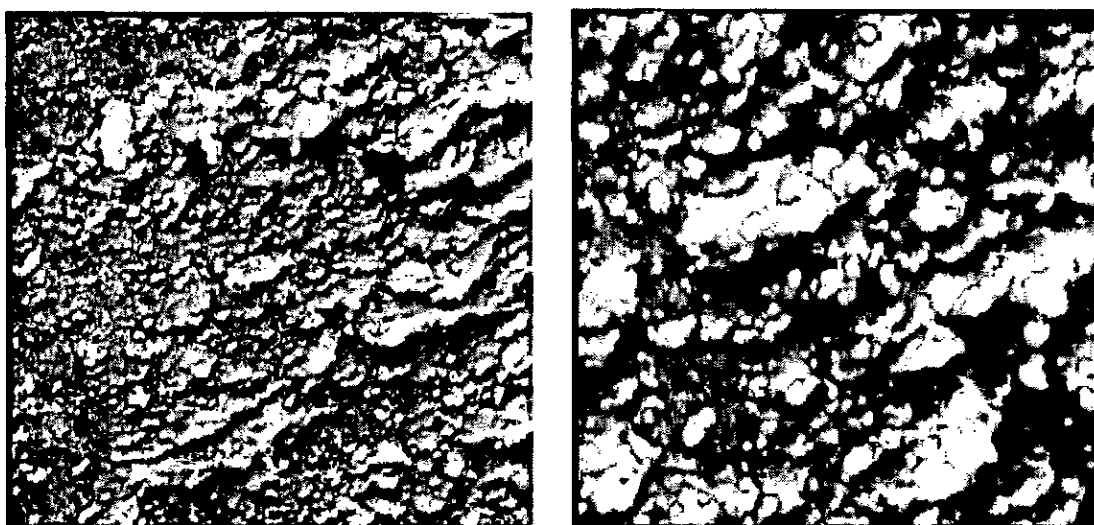


Fig 6. SEM images of Fe<sub>3</sub>O<sub>4</sub> nanoparticles coated with HAS.

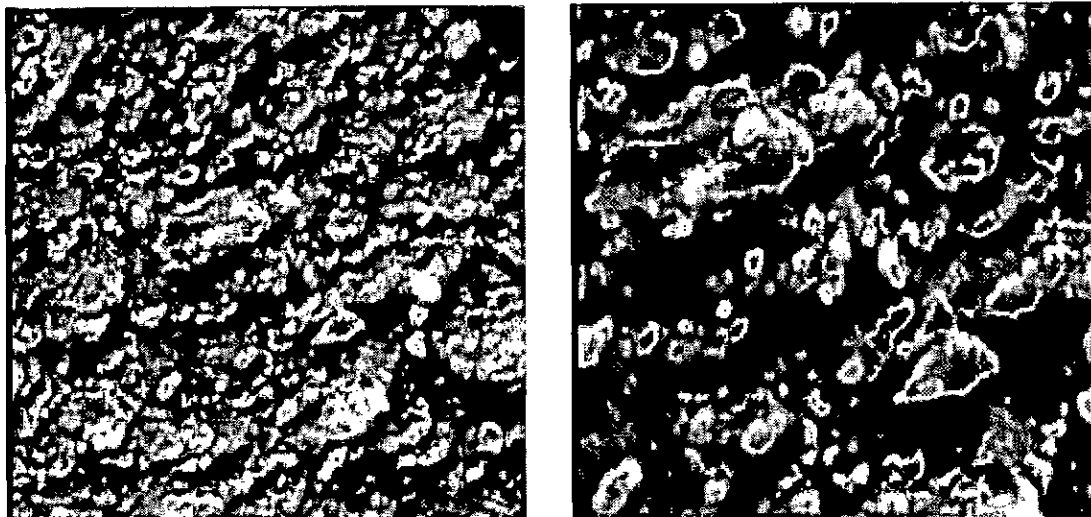


Fig 6. Continued.

### Infrared spectroscopy (FT-IR)

IR spectra were taken of KBr pellets formed from dry powder samples of iron oxide nanoparticles precursor, MNP-BSA and MNP-HAS, using a MIDAC M1200-SP3 spectrophotometer.

In the Fig.7(a) the peak at  $\sim 1595\text{cm}^{-1}$  and  $1480\text{cm}^{-1}$  are attributed to the CPC surfactant and in the Fig.7(b) the peak at  $\sim 3520\text{cm}^{-1}$  is attributed to the stretching vibration of  $-\text{OH}$ ,

which is assigned to  $-\text{OH}$  absorbed by  $\text{Fe}_3\text{O}_4$  nanoparticles and The peak at  $\sim 588\text{cm}^{-1}$  is attributed to the Fe-O bond vibration of  $\text{Fe}_3\text{O}_4$ . In the Fig.8 (a) the peak at  $\sim 2900\text{cm}^{-1}$  and  $1480\text{cm}^{-1}$  are attributed to the CTAB surfactant and Fig.8 (b) is as like as fig. (b) and Fig.9 (b) consists the characteristic bands of the BSA or HSA protein at  $1640\text{cm}^{-1}$  and  $1500\text{cm}^{-1}$  that represents the coataion MNP with proteins and Fig.9 (a) is as like as fig.8 (b) [22, 23].

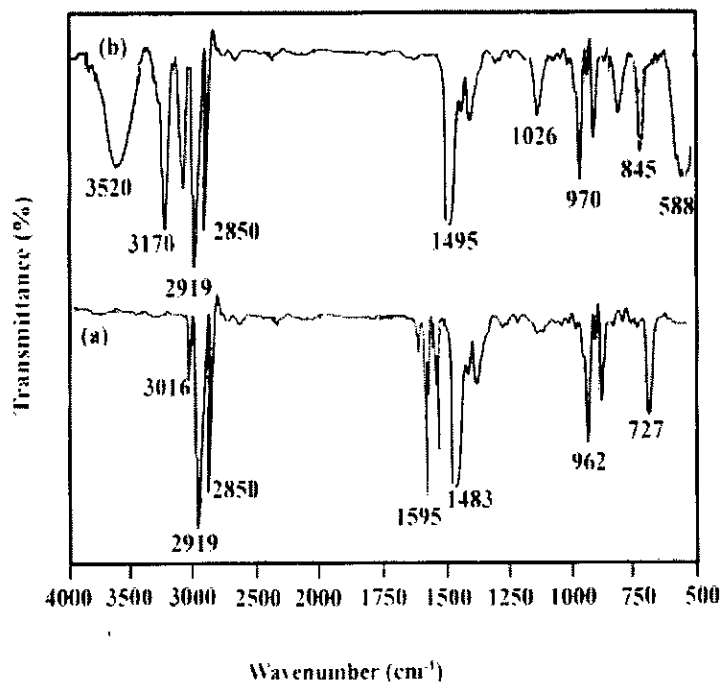


Fig 7. a) FT-IR spectra of CPC surfactant b) FT-IR spectra of  $\text{Fe}_3\text{O}_4$  nanoparticles prepared with CPC.

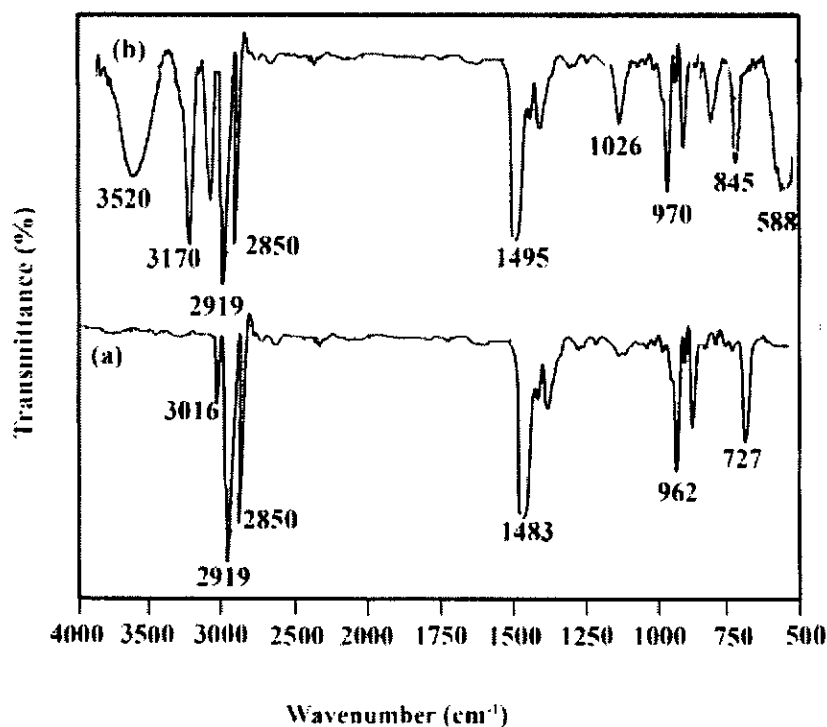


Fig 8. a) FT-IR spectra of CTAB surfactant b) FT-IR spectra of  $Fe_3O_4$  nanoparticles prepared with CTAB.

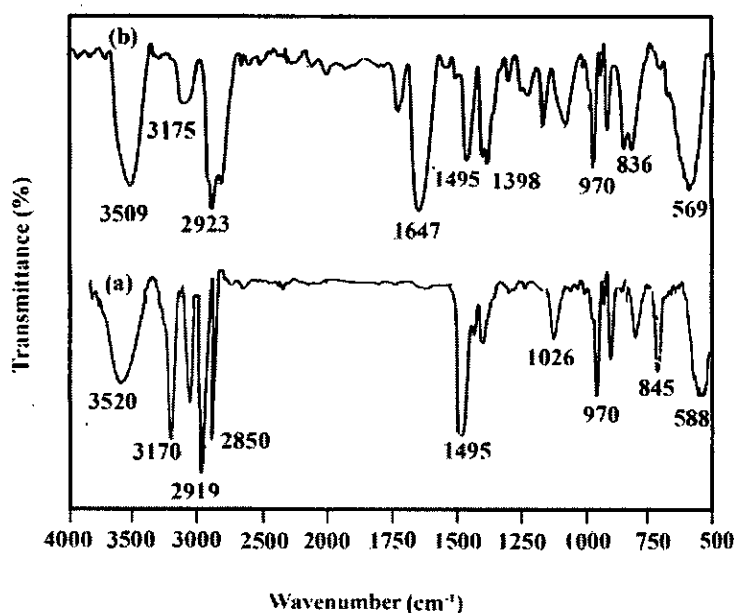


Fig 9. a) FT-IR spectra of  $Fe_3O_4$  nanoparticles prepared with CTAB b) FT-IR spectra of  $Fe_3O_4$  nanoparticles coated with BSA or HAS.

## RESULTS AND DISCUSSION

The energetic of BSA- nanoparticles or HSA- nanoparticles equilibrium can be conveniently characterized by three thermodynamic parameters, standard Gibbs free energy,  $\Delta G^\circ$  standard enthalpy,  $\Delta H^\circ$  and standard entropy

change,  $\Delta S^\circ$  can be calculated from the equilibrium constant,  $K$ , of the reaction using the relationship,  $\Delta G^\circ = -RT \ln K$ , in which  $R$  and  $T$  referring the gas constant and the absolute temperature, respectively. With respect Van't Hoff equation (1)

$$\frac{d \ln K}{d\left(\frac{1}{T}\right)} = \frac{-\Delta H^\circ}{R} \quad (1)$$

The Van't Hoff plot, lnK vs. 1/T, can be constructed

The Gives a liner plot of lnK versus 1/T,

The  $\Delta H^\circ$  can be calculated from the slope of the straight line,  $\frac{-\Delta H^\circ}{R}$  and the standard entropy

from equation (2)

$$\Delta S^\circ = \frac{\Delta H^\circ - \Delta G^\circ}{T} \quad (2)$$

All of the thermodynamic parameters for interaction of iron oxide nanoparticles, with BSA and HSA were calculate and reported in tables 4 and 5 respectively The Van't Hof plots are shown in Fig 9, 10.

**Table 4.** Thermodynamic parameters for interaction MNPs with BSA\*

T (K)	log K	Thermodynamic parameters		
		$\Delta H^\circ$ kJmol <sup>-1</sup>	$\Delta G^\circ$ kJmol <sup>-1</sup>	$\Delta S^\circ$ JKmol <sup>-1</sup>
293.15	3.444	17.041	-3.669	70.164
303.15	3.521	17.041	-3.853	68.919
313.15	3.622	17.041	-4.094	67.488

\*concentration of BSA= 10ppm and pH= 8, 9, 10, 11, 12

**Table 5.** Thermodynamic parameters for interaction MNPs with HSA\*

T (K)	log K	Thermodynamic parameters		
		$\Delta H^\circ$ kJmol <sup>-1</sup>	$\Delta G^\circ$ kJmol <sup>-1</sup>	$\Delta S^\circ$ JKmol <sup>-1</sup>
293.15	3.112	21.368	-3.315	83.621
303.15	3.231	21.368	-3.535	82.150
313.15	3.335	21.368	-3.770	80.271

\*concentration of HSA= 10ppm and pH= 8, 9, 10, 11, 12

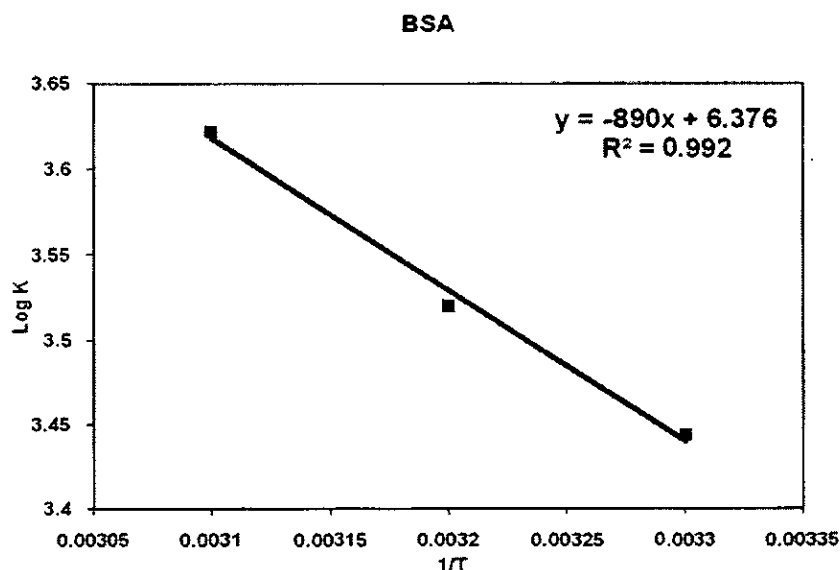


**Fig 10.** The Van't Hoff plot for interaction MNPs with BSA in various temperature.

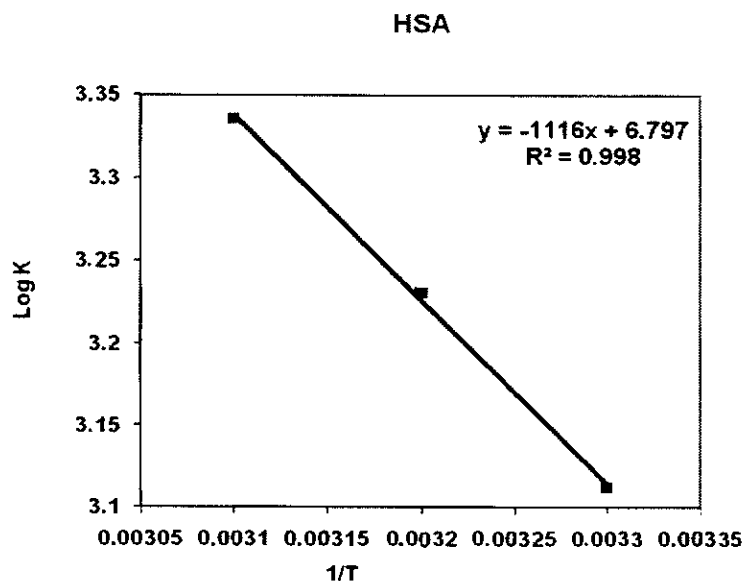


Fig 11. The Van't Hoff plot for interaction MNPs with HSA in various temperatures.

## CONCLUSIONS

Ultrafine, uniform, nearly spherical, and high purity  $\text{Fe}_3\text{O}_4$  nanoparticles could be prepared by the controlled chemical co-precipitation method. For this purpose, the solutions of ferrous/ferric were mixed with aqueous ammonium hydroxide ( $\text{NH}_3\cdot\text{H}_2\text{O}$ ) solution. The CTAB or CPC was chosen as the apt surfactant. The results show that  $\text{Fe}_3\text{O}_4$  nanoparticles can be produced in the sizes range of 8 to 20 nm by optimization of the operational parameters (concentration of surfactant, reaction temperature, solution pH, and stirring rate).

Carboxylate groups of BSA or HSA provide excellent ligation for iron oxide NPs. The presence of BSA or HSA on the NP surface was confirmed by FT-IR spectroscopy, SEM and XRD protein coated  $\text{Fe}_3\text{O}_4$  nanoparticles have excellent biocompatibility and low toxicity. The thermodynamic parameters of coating process represent to that both entropy and enthalpy parameters are driving forces.

## ACKNOWLEDGMENTS

We wish to express our gratitude to the Islamic Azad University of Shahreza for support this work.

## REFERENCES

- [1] M. B. Cortie, Gold Bulletin. 37 (1), (2004) 12.
- [2] P. Balaram, Current Science. 85(4), (2003), 421.

- [3] Ito, M. Shinkai, H. Honda, T. Kobayashi, J. Biosci. Bioeng., 100 (2005) 11.
- [4] O. Veiseh, J. W. Gunn, M. Zhang, Adv. Drug Deliv. Rev., 62 (2010) 284.
- [5] Agarwal, S. Saraf, A. Asthana, U. Gupta, V. K. Gajbhiye, N. Jain, International Journal of Pharmaceutics, 350 (2008) 3.
- [6] K. Gupta, M. Gupta, Biomaterials, 26 (2005) 3995.
- [7] P. Tartaj, M. D. Morales, S. Veintemillas. Verdaguier, T. Gonzalez-Carreño, C. Serna, J. Appl. Phys., 36 (2003) 182.
- [8] Y. E. Koo, G. R. Reddy, M. Bhojani, R. Schneider, Philbert, M. A. Rehemtulla, B. D. Ross, R. Kopelman, Adv. Drug. Del. Rev., 58 (2006) 1556.
- [9] Y. Zhang, N. Kohler, M. Q. Zhang, Biomaterials., 23 (2002) 1553.
- [10] S. Lubbe, C. Alexiou, C. Bergemann, Journal of Surgical Research, 95 (2001) 200.
- [11] S. Lubbe, C. Bergemann, J. Brock, D. G. McClure, J. Magn. Magn. Mat., 194 (1999) 149.
- [12] Lin, X. M.; Samia, A. C. S.; J. Magn. Magn. Mat. 305 (2006) 100.
- [13] H. Lu, E. L. Salabas, F. Schuth, Angewandte Chemie., 46 (2007) 1222.
- [14] S. Lee, et al, App. Phys. Lett., 79(20) (2001) 3308.

- [15] V. T Binh, et al, Appl. Surf. Sci., 130-132 (1998) 803.
- [16] J. Grabis, G. Heidemane, D. Rasmane, materials science (medziagotyra), 214 (2008) 292.
- [17] S. Jing, Z. Shaobing, P. Hou, Y. Yuan, W. Jie, L. Xiaohong, L. Mingyuan, Journal of Biomedical Materials Research, 13 (2006) 57.
- [18] K. D. Kim, S. S. Kim, Y. H. Choa, H. T. Kim, J. Ind. Eng. Chem., 13 (2007) 1137.
- [19] C.F. Zhang, J. Q. Cao, D. Z. Yin, Journal Applied Radiation and Isotopes, 61(6) (2004) 1255.
- [20] J. Flarakos, K. L. Morand, P. Vouros, J. Anal. Chem., 77 (2005) 1345.
- [21] H. W. He, H. J. Liu, K. C. Zhou, W. Wang, P. F. Rong, J. Cent. South Univ., Technol., 13 (2006) 6.
- [22] L. y Zhang, X. j. Zhu, H. w. Sun, G. r. Chi, J. x. Xu, Y. l. Sun, Current Applied Physics, 10 (2010) 828.
- [23] Samanta, H. Yan, N. O. Fischer, J. Shi, D. J. Jerry, V. M. Rotello, J. Mater Chem., 18(11) (2008) 1204.
- [24] Q. Yang, J. Liang, H. Han, J. Phys. Chem. B., 113 (2009) 10454.